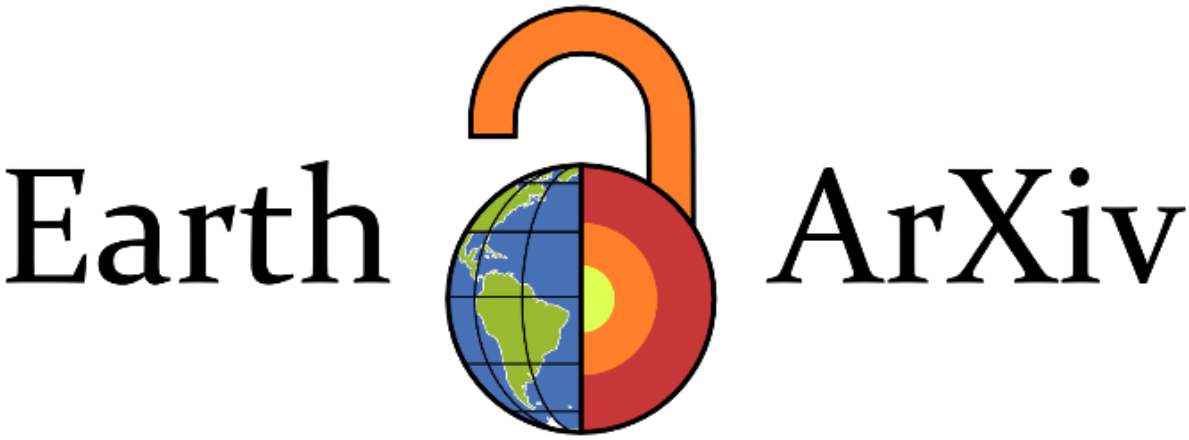

On the seasonal predictability of the 2020 North Atlantic tropical cyclone season

E. L. Levin[a] M. Chien,[b] E. A. Barnes,[b, c] H. He,[d] G. A. Vecchi,[d,e] W. Yang,[e]

[a] *Program in Atmospheric and Oceanic Sciences, Princeton University*

[b] *Faculty of Computing and Data Sciences, Boston University*

[c] *Department of Earth and Environment, Boston University*

[d] *High Meadows Environmental Institute, Princeton University*

[e] *Department of Geosciences, Princeton University*

Corresponding author: Emma Levin, emma.levin@princeton.edu

ABSTRACT: The 2020 Atlantic tropical cyclone (TC) season was unprecedented, producing a record storm count that exceeded the projected ranges of seasonal forecasts, despite their anticipation of above-normal activity. Here we assess the predictability of the extreme 2020 season from sea surface temperature (SST) forcing by examining a hierarchy of statistical, dynamical, and deep learning (DL) modeling frameworks, all constrained by observed SSTs. Although with observed SST forcing, physics-based models anticipated a relatively active season, the observed outcome lay beyond their ensemble ranges. To investigate this discrepancy, we first evaluate whether the large-scale environmental conditions of 2020 were conducive to the record-breaking activity. Although observed large-scale conditions in 2020 were generally favorable, they were not exceptionally so relative to other highly active seasons and did not indicate that a record-breaking season should have occurred. We next construct a 1,000-member ensemble using a DL model forced with observed SSTs to quantify the distribution of plausible outcomes. Using this large ensemble, the observed season emerges as a 0.5% event: highly unlikely, but not implausible. These results suggest that SST forcing provided only moderate predictive constraint, and that internal atmospheric variability could have played a role in the observed hyperactivity on top of the moderately favorable large-scale conditions. The inability of physics-based model ensembles to encompass the observed outcome does not indicate model failure or missing predictors, but reflects both limited predictability of the season from SST forcing and the inability of small ensembles to sample extreme tail risk.

SIGNIFICANCE STATEMENT: The 2020 Atlantic tropical cyclone (TC) season was the most active on record. Although seasonal forecasts anticipated above-normal activity, they did not encompass the observed hyperactivity. Even state-of-the-art physics-based, statistical, and deep learning (DL) models, when given "perfect" observed sea surface temperature (SST) inputs, did not capture the observed outcome within their simulated ranges. We assess how predictable this extreme season was from the observed SSTs. We show that while the large-scale conditions in 2020 were generally favorable for TCs, they were not exceptionally conducive to a record-breaking season. Using a 1,000-member DL ensemble forced with observed SSTs, we find that the 2020 season was an extremely rare but plausible outcome that a small ensemble could not have represented.

1. Introduction

Tropical cyclones (TCs) that form in the North Atlantic Ocean pose severe hazards to communities across the United States and the Caribbean (Young and Hsiang 2024; Weinkle et al. 2018; Klotzbach et al. 2018; Pielke et al. 2008). Accurate forecasts are therefore essential for preparedness and risk mitigation. Short-term weather forecasts, issued several days in advance, provide critical guidance for evacuation decisions and emergency response. In contrast, seasonal forecasts, issued before the onset of the hurricane season, aim to anticipate the overall characteristics of the upcoming season, particularly the range in possible storms that will form throughout the course of the season.

Many seasonal modeling and prediction systems rely on sea surface temperatures (SSTs) as a primary source of predictability. Atmosphere-only dynamical models, including both physics-based and deep learning (DL) approaches, can generate seasonal TC forecasts using predicted SSTs or extensions of pre-season SST anomalies as their boundary conditions (e.g., Chen and Lin 2013, 2011; Gao et al. 2019; Zhang et al. 2025a; Zhao et al. 2010). Similarly, retrospective experiments commonly force these models with observed SSTs to isolate the component of seasonal predictability attributable to ocean boundary forcing (e.g., Chan et al. 2021; Chien et al. 2025; Kortum et al. 2024; Levin et al. 2026; Zhao et al. 2009). Statistical and statistical-dynamical frameworks likewise use SSTs as predictors of seasonal TC activity (e.g., Eusebi et al. 2025a; Vecchi et al. 2011; Villarini et al. 2010). Although these approaches do not aim to reproduce the

exact storms that occurred, they provide physically plausible realizations of seasons consistent with the specified SST forcing.

The 2020 Atlantic TC season presents a striking test of this SST-based predictability framework. By many measures, the season was the most active on record, producing the highest number of long-duration TCs and tying the record for major hurricanes, while ranking second in hurricane count (Fig. 1). Although seasonal forecasts correctly anticipated above-normal activity, they substantially underestimated the magnitude of the hyperactivity. For example, NOAA's May 2020 outlook (`https://www.cpc.ncep.noaa.gov/products/outlooks/hurricane2020/May/hurricane.shtml`) projected 13–19 named storms, 6–10 hurricanes, and 3–6 major hurricanes, compared with the observed 30, 14, and 7, respectively.

Atmosphere-only dynamical models forced with observed monthly SSTs also failed to encompass the observed hyperactivity across their ensemble ranges. Two state-of-the-art models developed at the Geophysical Fluid Dynamics Laboratory (GFDL), HiRAM and AM2.5-C360, have demonstrated skill in simulating historical interannual and multidecadal Atlantic TC variability under observed SST forcing (Levin et al. 2026). Yet for 2020, despite simulating a moderately active season relative to the historical record, neither model's ensemble range (ten members for AM2.5-C360, and five members for HiRAM), captured the observed storm counts across any intensity category (Fig. 1). While observations occasionally fall outside ensemble spread in individual years (e.g., 1982 and 2013), as expected from internal variability (Vecchi and Villarini 2014), the 2020 season represents the most extreme discrepancy from the ensemble range in the historical record for long-duration TCs, and it was the only year where the observed count lay outside the ensemble range across all intensity bins. Although the 2020 season's activity was remarkable, such hyperactivity is not without precedent. Even the similarly hyperactive 2005 season fell within the simulated range of AM2.5-C360, with both models indicating strongly enhanced activity.

The inability of these dynamical models' ensemble range to capture the 2020 TC season when forced with observed SSTs raises a central question: to what extent was the hyperactive 2020 season predictable from the observed SST forcing? The inability of SST-forced models to capture the observed outcome across their ensemble spread could indicate deficiencies in the models or observational inputs, or it could instead reflect the intrinsic limits of predictability, with 2020

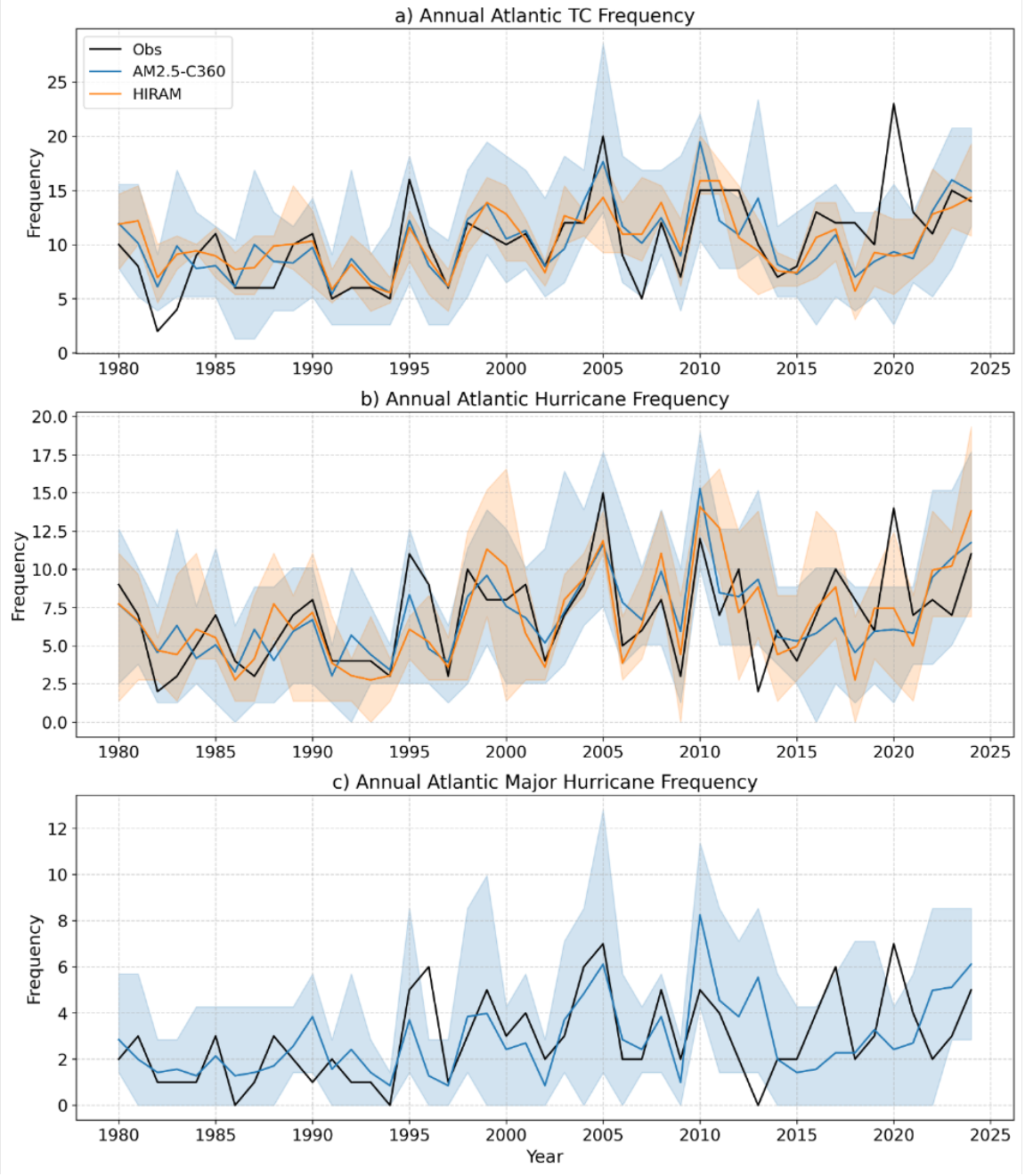

FIG. 1. Annual frequency of (a) TCs, (b) hurricanes, and (c) major hurricanes from 1980–2024. The observational record (black) is computed using the methodology and duration thresholds of Landsea et al. (2010a) to estimate the observed TC count in panel (a). Model simulations include AM2.5-C360 forced with observed and bias-corrected SSTs from Chan et al. (2021) (blue) and HiRAM forced with the same SSTs (orange). Shading denotes the full ensemble range (minimum–maximum) for each model (ten members for AM2.5-C360; five members for HiRAM), and solid lines indicate ensemble means. Panel (c) shows only AM2.5-C360 results, as HiRAM does not produce storms of sufficient intensity to be classified as major hurricanes.

representing a rare but dynamically plausible realization that a small ensemble size failed to sample. We evaluate these competing explanations through two broad hypothesis families:

The first family of hypotheses considers whether deficiencies in models or observational datasets contributed to the poor simulation of 2020 Atlantic TC counts. Within this framework, we assess the following possibilities:

1. Atmosphere-only models may exhibit structural limitations in their representation of TC formation, reducing their reliability in simulating interannual Atlantic TC variability.

2. Observed storm counts in recent decades, as shown in Fig. 1 (black lines), may be inaccurate.

3. Errors may be present in the observed monthly SST datasets used to force the models in 2020.

4. SST-forced models may not adequately represent the influence of observed aerosol changes on TC activity. Two major events in 2020 likely altered aerosol concentrations over the Atlantic basin. First, International Maritime Organization (IMO) regulations on the sulfur content of shipping fuel took effect on 1 January 2020, reducing maximum sulfur content from 3.5% to 0.5%. Implemented to improve air quality, this policy reduced aerosol loading over the oceans and altered regional radiative fluxes (Diamond 2023; Jordan and Henry 2024; Zhang et al. 2025b). Second, the onset of the COVID-19 pandemic led to substantial reductions in global emissions. Previous work suggests that decreased aerosol concentrations over North America and Europe can be associated with enhanced Atlantic TC activity (Murakami 2022, 2024). Because the SST-forced simulations analyzed here employ prescribed CMIP5 aerosol forcings rather than observed 2020 aerosol fields, the combined radiative and dynamical effects of these aerosol perturbations may not be represented.

The second hypothesis family considers the possibility that the hyperactive 2020 season was a highly unlikely, but dynamically plausible, realization of the internal variability of the climate system that could not have been captured by the small ensemble sizes of the GFDL models. Under this interpretation, the large-scale environmental conditions in 2020 may have permitted a wide range of outcomes, including a low-probability hyperactive season, but there would have been limited predictability from the monthly mean observed SST forcing. Subseasonal variability and internal atmospheric fluctuations could have amplified activity beyond the ensemble mean response, leading to an outcome that was not well captured by the small ensemble size of the

models. To fully address this second family of hypotheses, this paper seeks to answer the following research questions:

1. Was the 2020 season an extreme tail event in the small AM2.5-C360 and HiRAM ensembles whose likelihood could only be quantified by a very large calibrated ensemble?

2. To what extent could the hyperactive 2020 TC season have been predictable from the observed monthly SST forcing?

In the following sections we apply statistical analyses, dynamical diagnostics, DL–based climate simulations, and a theoretical framework to evaluate the two competing hypothesis families and the posed research questions. The evidence presented in this paper suggests that the 2020 season was a low-probability outcome, rather than a structural failure in the models or observational record. Our results suggest that the observed 2020 SST forcing provided limited predictability for the extreme hyperactivity that occurred, with the observed season representing a tail outcome that was not sampled by the relatively small GFDL ensembles. At the same time, we cannot exclude the possibility that additional mechanisms not examined in this paper influenced the 2020 season.

2. Methods and data

a. Dynamical Models

To place the 2020 Atlantic TC season in the context of recent historical variability, we generate a multi-ensemble record of TC, hurricane, and major hurricane activity using two global TC-permitting atmospheric models developed at GFDL: AM2.5-C360 and HiRAM (Zhao et al. 2009). Following the methods of Levin et al. (2026), we conducted multi-ensemble historical experiments with both models. We generated ten (five) ensemble members for AM2.5-C360 (HiRAM), each forced with bias-corrected observed monthly SSTs from the HadISST dataset (Chan et al. 2021) over the period 1980–2024. From these simulations, we compute annual counts of TCs, hurricanes, and major hurricanes to construct a modeled range of historical Atlantic TC activity.

To evaluate hypothesis 4 from Section 1, which proposes that the 2020 reduction in atmospheric aerosols was not represented in the SST-forced simulations, we conduct additional experiments. We generate a five-member ensemble of AM2.5-C180 (a slightly lower-resolution configuration of AM2.5-C360 with approximately 50-km grid spacing) spanning 1980–2024. In these simulations,

the model is forced with observed aerosol fields from the MERRA-2 reanalysis (Gelaro et al. 2017), rather than the CMIP5 aerosol reconstructions used in the historical integrations. This experiment isolates the effect of realistic interannual aerosol variability on modeled TC counts.

As a second approach, we perform an idealized modeling experiment to obtain additional samples and better quantify the relationship between sulfate and black carbon aerosols and Atlantic TC activity. Using the HiRAM model, we perform four simulations to isolate the effects of sulfate aerosols, which declined markedly in 2020 following the implementation of the IMO shipping regulation, and black carbon, which also decreased in 2020 due to reduced industrial activity and travel during the COVID-19 pandemic.

We perform a control experiment (cntl) in which the model is forced by the annual cycle of SSTs averaged over the period 1986–2005, following the methodology of Vecchi et al. (2019). This climatological SST cycle is repeated for 200 years following a 10-year spin-up, such that the 200-year mean represents the model's steady-state climatological baseline. We then perform three additional experiments using the same SST forcing as the control. In the first experiment, sulfate aerosols are removed over the North Atlantic (zeroSO4NA), and the model is integrated for 50 years. In the second experiment, sulfate aerosols are removed globally (zeroSO4global), and the model is again integrated for 50 years. In the final experiment black carbon emissions are removed globally (zeroBCglobal), and the model is integrated over 50 years. This serves as an exaggerated analogue to the global reduction in black carbon brought on by the COVID-19 pandemic.

To identify TCs and seed disturbances in both models, we follow the tracking procedure described in Levin et al. (2026). Hurricanes are defined as TCs that attain maximum winds exceeding 33 m s^{-1} at least once during their lifetime. Major hurricanes are identified in AM2.5-C360 as storms whose maximum winds exceed 45 m s^{-1}, a threshold slightly lower than the observed 50 m s^{-1} standard because the model rarely produces storms at the observed major hurricane intensity. HiRAM does not reliably simulate storms of sufficient intensity to meet this major hurricane threshold, and therefore major hurricane statistics are reported only for AM2.5-C360.

b. Statistical-Dynamical Model

To characterize the range of plausible seasonal Atlantic TC counts over the recent historical period (1980–2024), we employ the statistical–dynamical model of Vecchi et al. (2011) that uses

monthly SST data as an input and source of seasonal TC predictability. This framework estimates the expected annual Atlantic TC count, λ, using a Poisson regression in which λ depends solely on SST. λ is modeled as a function of the mean seasonal SST anomaly in the Atlantic main development region (MDR) and the mean seasonal SST anomaly across the tropics, since these two predictors together have been shown to be a robust indicator of Atlantic TC activity in the present climate (Vecchi and Soden 2007; Villarini et al. 2011; Eusebi et al. 2025b). Specifically, the logarithm of λ is modeled as the following linear function:

$$\lambda = \exp\left(1.707 + 1.388, SST_{MDR} - 1.521, SST_{TROP}\right), \tag{1}$$

where SST_{MDR} and SST_{TROP} are defined relative to the 1982–2005 climatology. The coefficients of Equation 1 have not been updated from those of Vecchi et al. (2011). The MDR is defined as 10°–25°N, 80°–20°W, and the tropical mean spans 30°S–30°N.

This formulation provides a full probabilistic distribution of seasonal outcomes conditional on the SST state. Thus, for each year in 1980–2024, the model yields a distribution of possible TC counts. We use this distribution to quantify the percentile rank of the observed 2020 season relative to SST-forced expectations.

We further use this model to evaluate hypothesis 3 from Section 1, which posits that discrepancies between observed and simulated 2020 TC counts may arise from inconsistencies in the observed SST datasets used to force atmosphere-only models. The AM2.5-C360 and HiRAM simulations analyzed here (Section a) are forced with a corrected version of the HadISST dataset (Chan et al. 2021). To assess the sensitivity of the inferred TC distribution to the choice of SST product, we apply the statistical–dynamical model separately using three independent SST datasets: the Optimum Interpolation Sea Surface Temperature dataset (OISST; Huang et al. (2021)), the Hadley Centre Global Sea Ice and Sea Surface Temperature dataset (HadISST; Schneider et al. (2013)), and the Extended Reconstructed Sea Surface Temperature dataset (ERSST; Huang et al. (2017)).

c. DL-based Model

Although the multi-ensemble historical integrations with AM2.5-C360 and HiRAM provide a dynamical range of Atlantic TC outcomes and require substantial computational resources, this

study questions whether their ensemble sizes of ten and five members, respectively, are= too small to fully characterize the probabilistic distribution of plausible 2020 seasonal outcomes.

Recent advances in DL weather models have shown substantial promise for simulating TCs. Once trained, these models can be integrated efficiently with significantly lower computational costs compared to traditional dynamical models like AM2.5-C360 and HiRAM (e.g. (Bi et al. 2023; Chen et al. 2023; Lam et al. 2023; Lang et al. 2024; Kochkov et al. 2024). In this study, we employ the Ai2 Climate Emulator version 2 (ACE2; Watt-Meyer et al. (2025)) to perform multi-ensemble annual simulations of historical Atlantic TC seasons, including 2020. We use a version of ACE2 trained on the ERA5 reanalysis (Hersbach et al. 2020). Previous studies have demonstrated that ACE2 is numerically stable over simulations spanning hundreds to thousands of years (Watt-Meyer et al. 2025) and can realistically reproduce TC characteristics across subseasonal to interannual timescales (Chien et al. 2025). These properties make ACE2 a robust platform for generating large ensembles of Atlantic TC seasons and for investigating the range of plausible outcomes for extreme events such as the 2020 season.

We generate a 1,000-member SST-forced ensemble for each year during 2005–2020 (including the anomalously active 2005 and 2010 seasons) and for the anomalously inactive 1982 season. Following Chien et al. (2025), ensemble members for a given year are generated by repeatedly integrating the ACE2 model under identically fixed SST boundary forcing. For a given target year (e.g., 2020), observed SSTs from that year are prescribed and repeated cyclically. The model is then integrated autoregressively for 100 consecutive years under these repeating SST boundary conditions. Each simulated year represents one dynamically distinct realization of the same SST-forced year and is treated as an independent ensemble member.

To obtain 1,000 members efficiently, we perform ten parallel integrations ("chunks"), each producing 100 ensemble members via the 100-year repeated-SST integration described above. Distinct initial atmospheric states are used for each chunk. Specifically, we initialize ACE2 from publicly available initial conditions and integrate the model forward for one year using SST boundary conditions from the year preceding the target year (e.g., 2019 SSTs when constructing the 2020 ensemble). The final model state from this spin-up integration is then used to initialize one 100-year repeated-SST chunk. This procedure is repeated to generate ten distinct initial conditions, yielding $10 \times 100 = 1{,}000$ ensemble members. Because SST boundary conditions are held fixed

within each ensemble while atmospheric initial conditions differ, the resulting spread reflects internal atmospheric variability under identical SST forcing. This design allows us to quantify the distribution of plausible seasonal TC outcomes conditioned on the observed SST state.

To detect TCs in ACE2, we follow the methodology of Chien et al. (2025) and Watt-Meyer et al. (2025), utilizing the TempestExtremes framework (Ullrich and Zarzycki 2017). By generating a 1,000-member ensemble for the 2020 season, we can robustly estimate the percentile rank of the observed 2020 storm count within the modeled distribution and to characterize the tail behavior of seasonal variability. In doing so, we can assess whether the observed hyperactivity represents a statistically rare but dynamically plausible realization, consistent with the second family of hypotheses outlined in Section 1.

d. Theoretical Framework

To assess whether the large-scale environmental conditions in 2020 were favorable for a hyperactive Atlantic season, we apply the theoretical framework of Hsieh et al. (2020) to ERA5 reanalysis data (Hersbach et al. 2020) over the period 1980–2024.

The framework conceptualizes TC formation as a two-stage process involving precursor seed disturbances and subsequent development into fully formed TCs. Under this formulation, the annual number of North Atlantic TCs, N_{TC}, is approximated as

$$N_{TC} \approx SPI \times P(\Lambda), \tag{2}$$

where SPI is the seed propensity index, a proxy for the number of precursor seed disturbances, and $P(\Lambda)$ is a proxy for the nondimensional probability that a seed disturbance develops into a TC. The seed propensity index is defined as

$$SPI = (-\omega) \cdot \frac{1}{1 + Z^{-1/\sigma}}, \tag{3}$$

where

$$Z = \frac{f + \zeta}{\sqrt{|\beta + \partial_y \zeta| U}}. \tag{4}$$

The variable ω is the 500 hPa pressure coordinate vertical velocity ($\omega < 0$ for upward motion), $\sigma = 0.69$ is a nondimensional fitting parameter, and Z is nondimensional variable that represents low level vorticity spinup. f is the Coriolis parameter, β is its meridional gradient, ζ is 850 hPa relative vorticity, and U is a constant wind speed of 20 m/s which is empirically fit in Hsieh et al. (2020).

Next, $P(\Lambda)$ is defined as

$$P(\Lambda) = \frac{1}{1 + (\Lambda_0/\Lambda)^{1/\gamma}}, \tag{5}$$

where

$$\Lambda = \frac{\nu_s \cdot \chi}{PI}. \tag{6}$$

The variables $\Lambda_0 = 0.014$ and $\gamma = -0.9$ are dimensionless fitting parameters, and Λ denotes the ventilation index (Tang and Emanuel (2010); Tang and Emanuel (2012)). ν_s is vertical wind shear between 250 hPa and 850 hPa, PI is potential intensity, and χ is a dimensionless variable representing entropy deficit.

In this study, we extend the existing framework by incorporating monthly mean data from ERA5, averaged over the tropical Atlantic (10°–30° N) during June through November, to derive a proxy for TC activity. Basin-wide means are calculated over a region extending beyond the Main Development Region (10°–25° N, 80°–20° W) to include the Gulf of Mexico, in order to account for the high concentration of storms that occurred there in 2020 (Fig. S4). Including the Gulf of Mexico ensures that differences in TC track locations among years are appropriately represented in the analysis.

We also construct an alternative proxy for annual Atlantic TC counts that explicitly incorporates tracked precursor seeds. In this formulation, annual TC activity is approximated as

$$N_{TC} \approx N_s \times P(\Lambda), \tag{7}$$

where N_s denotes the observed annual count of explicitly tracked TC seeds. Here, seed frequency is diagnosed directly from reanalysis data, allowing us to more explicitly separate variability in seed frequency from variability in development probability.

3. Results

a. Testing the first hypothesis family

In this section, we present the results to evaluate the first family of hypotheses as to why the GFDL models poorly represented the hyperactive 2020 Atlantic TC season within their ensemble ranges: whether there were fundamental deficiencies in the models or observational datasets.

1) Hypothesis Number One

This hypothesis poses that the dynamical atmosphere-only models used in this study to generate the historical TC record in Figure 1 (AM2.5-C360 and HiRAM) may be limited in their ability to represent TC genesis, and thus, are unreliable to assess Atlantic TC interannual variability.

This explanation appears unlikely. In addition to the demonstrated skill of AM2.5-C360 and HiRAM in reproducing the long-term historical variability of Atlantic TC activity (Levin et al. 2026), the influence of SSTs on TC frequency and intensity (Chan et al. 2021), and the annual TC cycle (Yang et al. 2021), it is notable that the anomalous 2020 season also lies at or beyond the ensemble range in other independent modeling systems. Seasonal forecasts from physics-based coupled models such as GFDL SPEAR and FLOR (Murakami et al. 2025), as well as from DL-based models such as NeuralGCM (Zhang et al. 2025a), similarly place 2020 at the edge or outside their ensemble distributions. The fact that multiple structurally distinct modeling frameworks fail to encompass the observed 2020 hyperactivity within their ensemble spread suggests that a model-specific deficiency is unlikely to be the sole explanation.

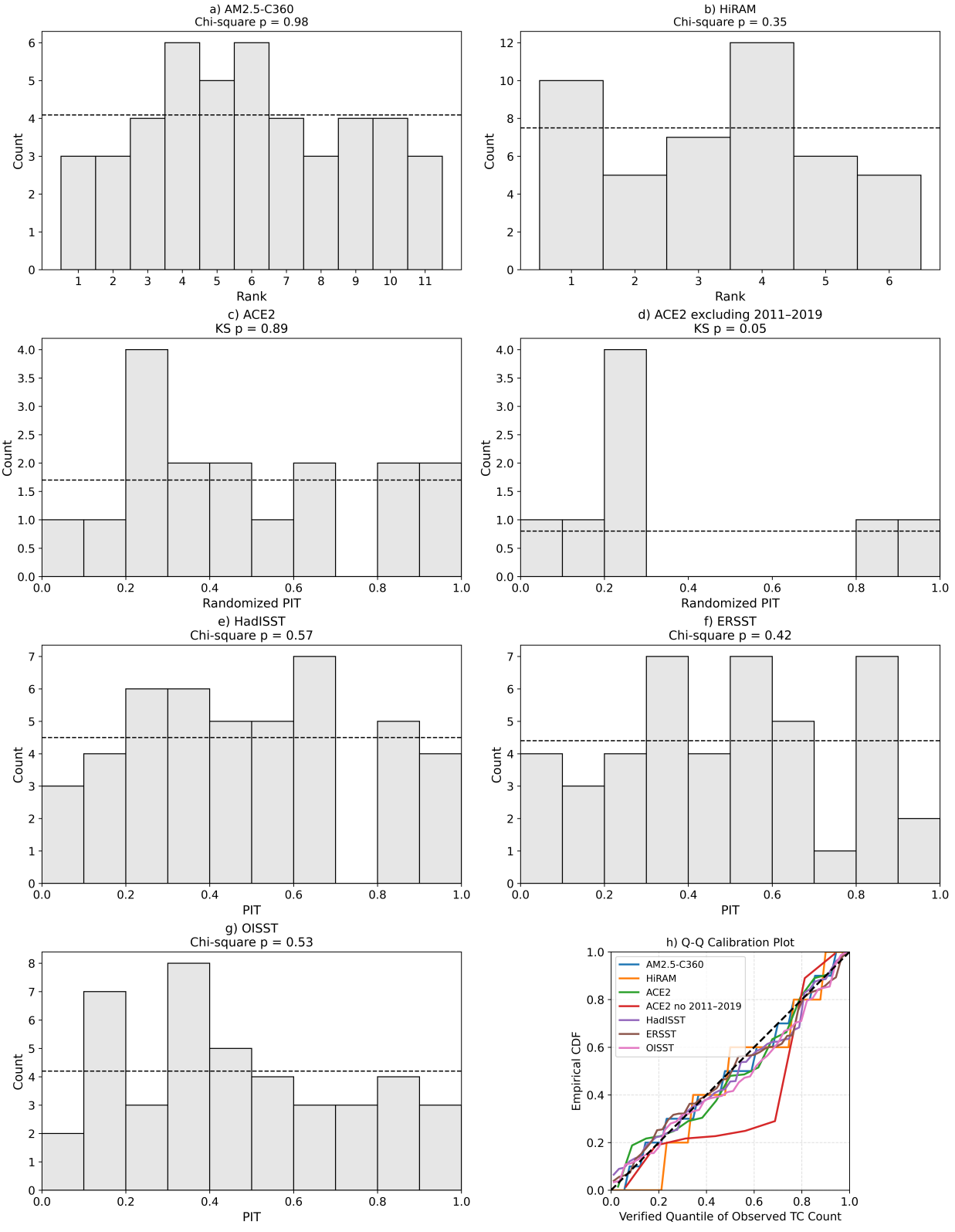
a) AM2.5-C360
Chi-square p = 0.98
Count
Rank
b) HiRAM
Chi-square p = 0.35
Count
Rank
c) ACE2
KS p = 0.89
Count
Randomized PIT
d) ACE2 excluding 2011–2019
KS p = 0.05
Count
Randomized PIT
e) HadISST
Chi-square p = 0.57
Count
PIT
f) ERSST
Chi-square p = 0.42
Count
PIT
g) OISST
Chi-square p = 0.53
Count
PIT
h) Q-Q Calibration Plot
AM2.5-C360
HiRAM
ACE2
ACE2 no 2011–2019
HadISST
ERSST
OISST
Empirical CDF
Verified Quantile of Observed TC Count

FIG. 2. Reliability diagnostics for the modeling systems used in this study against the observed seasonal Atlantic TC counts computed using the methodology of Landsea et al. (2010a). Panels (a) and (b) show rank histograms for AM2.5-C360 (10-member ensemble) and HiRAM (5-member ensemble), respectively, forced with observed SSTs over 1980–2024 (n=45 years). For these relatively small discrete ensembles, calibration is assessed using rank histograms, with the p-values from Chi-square goodness-of-fit tests against the uniform distribution shown in the subplot titles. Panels (c) and (d) show randomized probability integral transform (PIT) histograms for the 1,000-member ACE2 DL ensemble for 1982 and 2005–2020 (n=17) and for the same years excluding the model training period (2011–2019; n=8), respectively. Because ACE2 produces a very large ensemble and the outcome variable is discrete count data, randomized PIT values are used instead of rank histograms. Given the limited sample sizes for ACE2, calibration is assessed using Kolmogorov–Smirnov (KS) tests against the uniform distribution. Panels (e)–(g) show randomized PIT histograms for the statistical-dynamical model of Vecchi et al. (2011) forced with HadISST (1980–2024, n=45), ERSST (1980–2023, n=44), and OISST (1981–2022, n=42), respectively. Because these models produce full probabilistic distributions, PIT diagnostics are used; Chi-square goodness-of-fit tests against the uniform distribution are shown in the subplot titles. In panels (a)–(g), the dashed horizontal black line denotes the expected histogram frequency under perfect calibration, for which the ranks or verification quantiles of the observed TC counts are uniformly distributed. Higher p-values indicate weaker evidence against uniformity. Panel (h) shows a Q–Q calibration diagnostic for all models in panels (a)–(g). For each verification year, the percentile at which the observed TC count falls within the corresponding forecast distribution is computed (using randomized PIT for discrete ensemble forecasts), yielding one verification quantile per year. The empirical distribution of these verification quantiles is then compared against the standard uniform distribution. A well-calibrated forecast system should produce verification quantiles that lie close to the 1:1 dashed black line.

Additionally, we assess the reliability of the historical AM2.5-C360 and HiRAM ensembles against observed seasonal Atlantic TC counts using rank histograms (Figures 2a,b; Hamill (2001); Gneiting et al. (2007)). While both histograms show a slight visual concentration near the center, which could qualitatively suggest mild underdispersion, chi-square goodness-of-fit tests against the uniform distribution yield high p-values ($p = 0.98$ for AM2.5-C360; $p = 0.35$ for HiRAM), providing no evidence to reject the null hypothesis of uniformity. This indicates that, over the historical record, the ensemble spread is broadly consistent with the observed distribution of seasonal TC counts. The Q–Q calibration diagnostic (Figure 2h) provides additional support, with

both models lying close to the 1:1 line, indicating that the observed TC counts fall at approximately uniformly distributed quantiles within the forecast distributions. Together, these diagnostics suggest that the GFDL ensembles are reasonably well calibrated over the historical period, despite failing to encompass the extreme 2020 season within their ensemble ranges.

2) Hypothesis Numbers Two and Three

The second hypothesis regarding the reliability of the TC observations appears unlikely, as the post-1980 Atlantic TC record is considered highly reliable given modern satellite, aircraft reconnaissance, and remote sensing observations, with confidence further enhanced in recent years by newer geostationary satellites. Additionally, this study uses the observed TC record computed using the methods of Landsea et al. (2010b), which excludes short-duration storms that may have been missed in earlier decades due to less advanced observing capabilities, thereby improving temporal homogeneity in the historical record. Moreover, the anomalous 2020 activity extended to hurricanes and major hurricanes, which are even less susceptible to detection ambiguity, making observational error an unlikely explanation for the model–observation discrepancy.

The third hypothesis suggests there are errors in the SST dataset used to force the atmosphere-only models. To test this, we apply the statistical–dynamical model of Vecchi et al. (2011), which predicts seasonal Atlantic TC activity from SST, using three independent SST products: OISST, HadISST, and ERSST. The PIT histograms for the resulting seasonal TC distributions (Fig. 2) show no statistical evidence of deviation from uniformity based on chi-square tests, indicating that these statistical-dynamical reconstructions are well calibrated. The corresponding time series of the statistical-dynamical models (Fig. S1) capture substantial interannual variability, with correlations of $r = 0.66$–0.70 against observations. Despite known differences among SST datasets in their long-term trends (Menemenlis et al. 2025), the predicted 2020 TC distributions are nearly identical, with ensemble means ranging from 10.9 to 11.8 storms. This provides no evidence that errors in HadISST, which forces the dynamical simulations, explain the discrepancy.

3) Hypothesis Number Four

Our fourth hypothesis suggests that the failure of the observed 2020 TC count to fall within the AM2.5-C360 and HiRAM ensemble ranges reflects limitations of SST-forced models in representing the impacts of abrupt aerosol perturbations. To test this, we use two approaches. First,

we perform a five-member AM2.5-C360 ensemble simulation over 1980–2024 using observed reanalysis-based aerosol concentrations, rather than the prescribed CMIP5 aerosol forcing used in the historical simulations shown in Fig. 1. Even when forced with observed aerosol concentrations, the model simulates 2020 as only a moderately active season (Fig. S2). The absence of a change in simulated Atlantic TC activity when including observed aerosols suggests that any radiative or dynamical effects associated with the 2020 aerosol reduction were either small or already reflected indirectly in the observed SST boundary conditions.

Additionally, we conduct idealized sensitivity experiments in which sulfate and black carbon aerosols are substantially reduced to emulate an exaggerated analogue of the 2020 aerosol decline. The resulting annual Atlantic TC count distributions are similar to the control, with all experiments producing approximately 12 TCs per year (Fig. S3). Kolmogorov–Smirnov tests show no statistically significant differences from the control in any experiment ($p = 0.28$–0.99), suggesting that, within this modeling framework, the direct radiative effects of prescribed low-frequency (>monthly) aerosol variations do not exert a robust influence on Atlantic TC activity. This does not preclude aerosol effects operating through SST-mediated pathways or synoptic-scale interactions, which are not represented in these experiments.

b. Testing the second hypothesis family

In this section, we evaluate the second hypothesis family, which considers the possibility that the hyperactive 2020 season was a highly unlikely but dynamically plausible outcome that could not have been captured by the small ensemble sizes of the AM2.5-C360 and HiRAM models.

1) Analysis of ensemble size

We first examine the historical ensembles from the dynamical AM2.5-C360 and HiRAM models shown in Fig. 1. Rather than treating 2020 in isolation, we quantify how often the observed storm count falls outside the modeled ensemble spread across the entire 45-year record.

Because the dynamical ensembles appear well calibrated (Fig. 2), the observed record can be interpreted as an additional equally likely realization drawn from the same distribution as the model ensemble members. Under this assumption, AM2.5-C360 (HiRAM) contains eleven (six) realizations per year, comprising ten (five) model members plus the observational record. The

probability that the observation lies outside the modeled ensemble range, is either the minimum or maximum of the combined set, is therefore

$$P(\text{outside ensemble range}) = \frac{2}{n}.$$

Therefore, the resulting annual exceedance probabilitiesare $2/11 \approx 0.18$ for AM2.5-C360 and $2/6 = 0.33$ for HiRAM, corresponding to expected exceedance counts over 45 years of approximately eight and fifteen, respectively.

In Fig. 1, the observed record lies outside the AM2.5-C360 ensemble spread six times for total TCs, three times for hurricanes, and five times for major hurricanes. These outcomes are well within sampling variability and are therefore consistent with a calibrated system. Similarly, for HiRAM, the observed record lies outside the ensemble spread fifteen times for TCs and twelve times for hurricanes, both close or equal to the expectation of fifteen exceedances.

Thus, even in a well calibrated system with only five to ten ensemble members, it is expected that the observation will fall outside the ensemble range multiple times over a 45-year period. Although 2020 stands out visually because it lies outside the ensemble spread simultaneously for TCs, hurricanes, and major hurricanes, similar exceedances occur elsewhere in the historical record (e.g., 2013 and 1996). Therefore, this analysis supports the conclusion that the small ensemble sizes of AM2.5-C360 and HiRAM could have been inadequate to capture the extremely hyperactive 2020 season.

At the same time, the limited ensemble sizes of AM2.5-C360 and HiRAM constrain our ability to precisely estimate tail probabilities of extreme events like the 2020 season. This limitation motivates the use of the 1,000 member ACE2 DL–based model ensemble and the statistical-dynamical model from Vecchi et al. (2011) to generate a full distribution of seasonal TC counts and more robustly characterize the distribution's tail behavior. The ACE2 1,000 member ensemble spans 1982 and 2005-2020, encompassing both active and inactive seasons that are captured within the ensemble spread of dynamical models, including 1982, 2005, 2009, and 2010 (Fig. 1). Our comparison across years in the recent record allows us to assess whether the behavior of the DL–based model diverges substantially from that of physics-based atmosphere-only models.

The observed annual TC counts and the distribution of simulated TC counts from the 1,000-member historical ACE2 ensemble are shown in Fig. 3. ACE2 exhibits a moderate positive

correlation between the observed TC counts and the ensemble-mean simulated counts ($r = 0.62$), indicating skill in distinguishing between relatively active and inactive seasons due to SST and carbon dioxide external forcing alone. The ensemble mean peaks during active seasons such as 2005 and 2010, and shows local minima during inactive seasons such as 2009 and 2014, consistent with the observed variability.

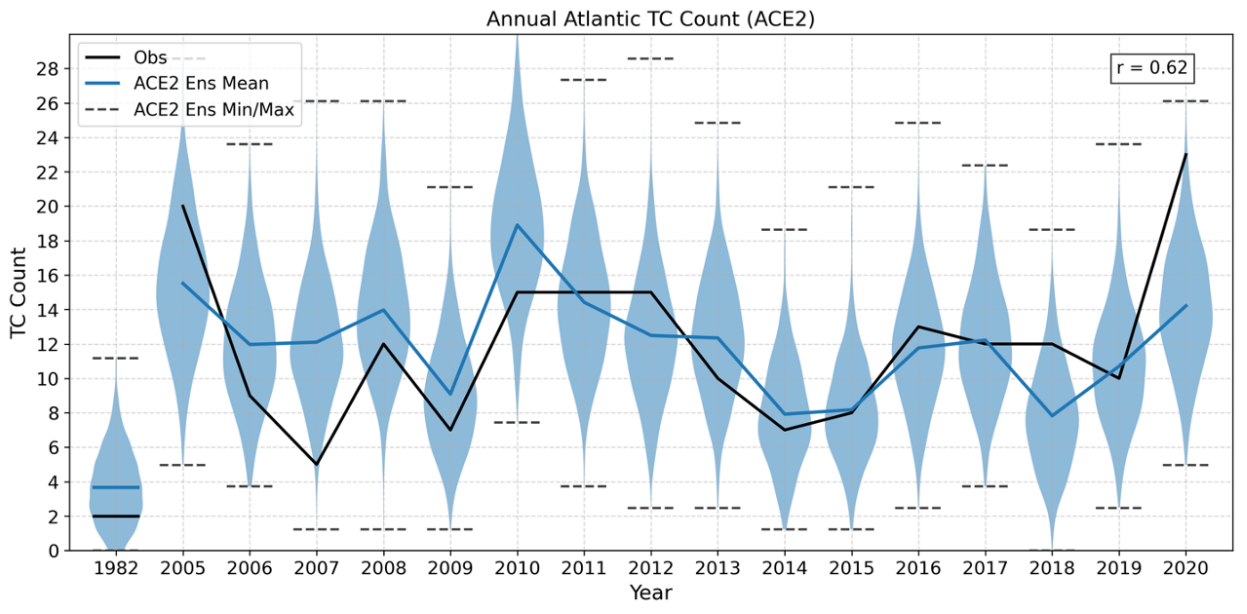

FIG. 3. Annual Atlantic TC counts for 1982 and 2005–2020. The adjusted observational record computed using the methods from Landsea et al. (2010a) is shown in black. Blue violin plots depict the distribution of simulated TC counts from the 1,000-member ACE2 ensemble forced with observed SSTs, with the ensemble mean indicated by the solid blue line, and ensemble minimum and maximum indicated by the dashed dark gray lines. The correlation between the ensemble-mean TC frequency and the observed counts is shown in the upper-right corner.

Beyond reproducing the observed mean-state variability, the ensemble exhibits substantial interannual spread. For each of the seventeen seasons shown, the simulated range of TC counts (the difference between the ensemble minimum and maximum) spans roughly ten to 26 storms. For instance, in 2005 the ensemble indicates that between approximately five and 28 TCs were dynamically plausible, whereas in the relatively inactive 2014 season the simulated range extends from one to nineteen TCs. Despite this considerable variability, the observed TC count falls within

the ensemble distribution for most seasons in the historical record. Furthermore, the randomized PIT histogram for the full ACE2 record (Fig. 2c) is not statistically distinguishable from uniform according to the K–S test, and the corresponding Q–Q plot lies close to the 1:1 line (Fig. 2h), indicating that the ensemble dispersion provides a realistic representation of seasonal uncertainty. In other words, the verifying observational quantile is approximately uniformly distributed across years, suggesting that the ensemble dispersion realistically represents seasonal uncertainty.

ACE2's performance is not uniform across all years, however. Visual inspection of Fig. 3 suggests that discrepancies between the ensemble mean and observations are largest prior to 2010 and in 2020, while agreement improves during 2010–2019. Additionally, the randomized PIT histogram for the subset of out-of-sample years (Fig. 2d,h) appears U-shaped, with a marginal K–S test p-value of 0.05 and the largest departures from the 1:1 line in the Q–Q plot, suggestive of reduced calibration. However, this subset contains only eight years, limiting statistical confidence. These years with the weaker reliability span the out-of-sample validation period, since the model's training includes 2011–2019 (Watt-Meyer et al. 2025). These results suggest stronger performance during in-sample years than in true out-of-sample evaluation.

There are several years in which the observed TC count falls near the extreme tails of the ACE2 ensemble distribution. One such case is 2007, an anomalously inactive season with only five observed TCs. The 1,000-member ACE2 ensemble, forced with observed 2007 SSTs, simulated a plausible range of approximately one to 26 storms, with an ensemble mean of twelve. Only fifteen of the 1,000 members produced five or fewer TCs, indicating that the realized season corresponds to a 1.5% lower-tail event within the modeled distribution. Although the ACE2 ensemble mean represented 2020 as a relatively active season, with the ensemble mean being third highest across the years in 3, below only 2005 and 2010, the observed 2020 hyperactivity verified at the extreme tail of the ACE2 ensemble distribution. The ensemble simulates a mean of approximately fourteen TCs (Table 1), compared to the 23 storms observed. Only 37 ensemble members produce at least 20 storms (3.7%), and just five members simulate 23 or more storms (0.5%). Thus, under the observed 2020 SST forcing, ACE2 characterizes the realized season as a rare but physically plausible outcome, verifying at the 99.5th percentile of the modeled distribution.

Table 1 compares the estimated likelihood of the 2020 hyperactive season from the 1,000-member ACE2 ensemble distribution with that derived from the statistical–dynamical Poisson

TABLE 1. Modeled distribution of 2020 seasonal TC counts using a statistical-dynamical model with three SST products as inputs and the DL-based ACE2 1,000-member ensemble model. For each modelled TC count distribution we show the distribution's mean, quantile at which the observed 23 TC counts in 2020 verified against the modeled distribution, and the corresponding percent of such an event.

Model	Model Mean TC count	Verified Quantile	Event Percent
Statistical-Dynamical (HadISST)	11.0	0.999	0.1%
Statistical-Dynamical (ERSST)	11.8	0.997	0.3%
Statistical-Dynamical (OISST)	10.9	0.999	0.1%
ACE2 1,000 member ensemble	14.1	0.995	0.5%

model described in Eq. 1, forced separately with HadISST, ERSST, and OISST SST datasets. The statistical–dynamical model is shown to be well calibrated in Fig. 2, with PIT histograms that are statistically indistinguishable from uniform and Q–Q plots that closely follow the 1:1 line. Across all modeling frameworks, the results consistently indicate that the observed 2020 SST boundary conditions did not strongly favor such an exceptional season and provided limited predictability for a hyperactive outcome, with estimated probabilities of only 0.1–0.5% under the observed SST forcing.

Although a 0.5% event is highly unlikely in any single year, its occurrence over a multidecadal record is less implausible. Assuming independence between seasons, the probability of observing at least one 0.5% event over a 45-year period (e.g., 1980–2024) is

$$P(\text{At least one } 0.5\% \text{ event}) = 1 - (0.995)^{45} \approx 0.20. \tag{8}$$

Thus, an event with a 0.5% annual probability has roughly a 20% chance of occurring at least once in a 45-year historical record.

To evaluate how ensemble size influences the ability to capture the full range of plausible 2020 Atlantic TC outcomes, we conduct a resampling experiment using the 1,000-member ACE2 simulation of the 2020 season. From this ensemble, we randomly draw either ten or fifteen members without replacement and repeat this procedure 10,000 times. These sample sizes mimic the ensemble sizes typically used in physics-based seasonal forecasting systems, which often consist of only ten to fifteen members (e.g., Murakami et al. (2025)). For each resampled ensemble,

TABLE 2. The percentage of 10,000 resampled realizations of annual Atlantic TC counts from the ACE2 model that satisfy specific activity thresholds. Each realization is constructed by randomly selecting either 10 or 15 ensemble members from the 1,000 ACE2 simulations of the 2020 season, without replacement, and repeating this sampling process 10,000 times.

Criteria across all samples (%)	10 ensembles	15 ensembles
≥1 ens with at least 20 TCs	32.99%	44.96%
≥2 ens with at least 20 TCs	5.86%	12.06%
≥1 ens with at least 23 TCs	8.03%	11.51%
≥2 ens with at least 23 TCs	0.24%	0.56%
mean ≥ 12 TCs ('active season')	97.96%	99.62%
mean < 12 TCs ('inactive season')	2.04%	0.38%
mean ≥ 17 TCs ('$+1\sigma$ season')	0.65%	0.16%
mean ≤ 7 TCs ('-1σ season')	0.00%	0.00%

we evaluate whether specific activity thresholds are met (Table 2). In particular, we assess the probability that at least one or at least two members simulate (i) a season with ≥20 TCs (comparable to other hyperactive years such as 2005) and (ii) a season with ≥23 TCs, matching the observed 2020 count. We also classify seasons using the ensemble mean. An "active" season is defined as one with a mean ≥12 TCs, consistent with the 2005–2020 observed mean (approximately twelve storms). A ten-member (fifteen-member) ensemble contains at least one realization with ≥23 TCs in only approximately 8% (12%) of resampled cases, highlighting how unlikely it is for an outcome as extreme as the observed 2020 season to be represented in a small ensemble size.

2) LARGE-SCALE ENVIRONMENTAL CONDITIONS IN 2020

To evaluate if the hyperactive 2020 season was a highly unlikely but dynamically plausible realization of the climate system, we examine the large-scale environmental conditions that prevailed during that year. Internal atmospheric variability operating on subseasonal timescales could have amplified activity beyond what would be anticipated from seasonal-mean conditions alone.

To test this idea, we leverage ERA5 reanalysis data in combination with the theoretical TC proxy introduced by Hsieh et al. (2020), defined as $N_{\mathrm{TC}} \approx \mathrm{SPI} \times P(\Lambda)$, which approximates seasonal TC counts as a function of the large-scale environment. We compute the seasonally (June-November) and tropical Atlantic main develop region (MDR)-averaged TC proxy using monthly mean ERA5

inputs for the period 1980–2024 ($\mathrm{SPI} \times P(\Lambda)$, Fig. 4a). This framework reproduces a substantial portion of the observed interannual variability in Atlantic TC activity, yielding a correlation of $r = 0.65$ between observed and both proxy-derived TC counts. Thus, seasonal-mean large-scale environmental conditions explain much of the historical variability in Atlantic TC activity.

Although the TC proxy estimates the 2020 season to be moderately active across the entire historical record of Fig. 4 and a local maximum in favorability in the years surrounding it, the observed TC count substantially exceeds the proxy estimate. When the 2020 season is excluded, the correlation between the observed counts and the seasonal $\mathrm{SPI} \times P(\Lambda)$ (blue line) increases to $r = 0.70$. Deviations between the proxy and observations are also evident in the surrounding years, particularly from 2018 to 2021. These results indicate that, based on the combination of several key seasonally averaged large-scale conditions alone, 2020 did not appear exceptionally favorable for the record-breaking hyperactivity that occurred.

Additionally, we examine the individual components of $P(\Lambda)$, the proxy for the likelihood that a TC will develop from a seed disturbance, averaged seasonally (June–November) over the Atlantic MDR (Figs. 4b–d). In 2020, the thermodynamic variables, potential intensity and moist entropy deficit, were close to their 1980-2024 climatological means, with moist entropy deficit slightly less favorable than average. Similar behavior is found using ASO averages (Fig. S6), corresponding to the climatological peak of the Atlantic TC season. Vertical wind shear in 2020 was more favorable than average, but not exceptionally so relative to other active years. Several seasons, including 2005, 2010, 2011, 2012, 2016, 2023, and 2024, exhibited comparably or more favorable shear conditions. While Bell et al. (2021) reported that ASO vertical wind shear in 2020, based on NCEP/NCAR reanalysis, was the fifth lowest since 1980, our ERA5 analysis suggests the anomaly was less extreme: in addition to the years identified by Bell et al. (2021), we find that 2006, 2012, 2023, and 2024 also had lower ASO vertical wind shear than 2020 (Fig. S6). Thus, although the large-scale thermodynamic and dynamic environment in 2020 was generally conducive to TC activity, the combined seasonal-mean values of vertical wind shear, potential intensity, and moist entropy deficit do not support the expectation of a record-breaking season. This finding suggests that internal atmospheric variability likely amplified TC activity beyond what would be anticipated from mean conditions alone.

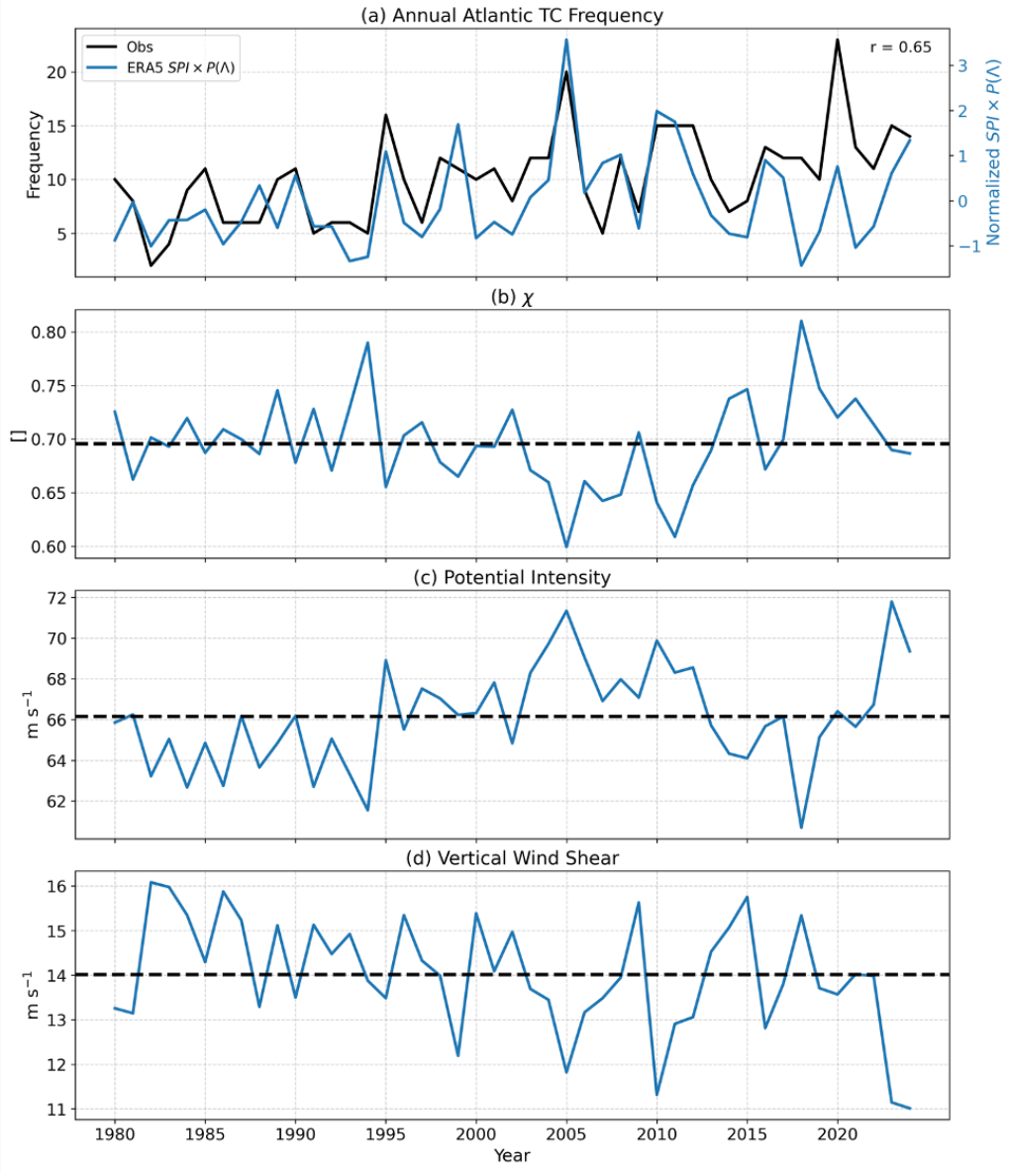

Fig. 4. a) Time series of observed annual Atlantic TC counts (black; left y-axis), approximated annual TC frequency (SPI $\times P(\Lambda)$; blue; right y-axis) derived from seasonally and TC main development region (MDR)-averaged monthly ERA5 data for 1980–2024. The parameterized TC frequencies are standardized using Z-score normalization, defined as $Z(x) = (x - \mu_x)/\sigma_x$, where x is the data point, μ_x is the mean over the full record, and σ_x is the standard deviation. The correlation coefficient between observed and approximated TC counts is shown in the upper-right corner of the panel. (b–d) Time series of the seasonal, MDR-averaged ERA5 environmental variables that contribute to the ventilation index (Eq. 6), a key control on TC genesis: (b) moist entropy deficit (lower values are more favorable for TC development), (c) potential intensity (higher values are more favorable), and (d) vertical wind shear (lower values are more favorable). Dashed black horizontal lines indicate the 1980–2024 climatological mean of each variable.

In addition to examining monthly mean large-scale environmental conditions relevant for TC development from a seed disturbance, we assess whether the abundance of seed disturbances themselves tracked at six-hourly intervals contributed to the hyperactive 2020 TC season emerging as a rare realization within the ensemble spread of multiple models. To do so, we examine explicitly tracked Atlantic TC seeds from three independent ERA5-based datasets (Moon et al. (2025); Vishnu et al. (2020); Ikehata and Satoh (2021)), in addition to our own tracking methodology. Each method tracks storms using six-hourly June-November North Atlantic ERA5 data. The resulting seed counts are shown in Fig. 5. These differing approaches yield different mean seed climatologies, yet they share broad interannual patterns. Notably, none identifies 2020 as a local maximum in seed count (Fig. 5). If the hyperactivity of 2020 were driven by anomalously many seeds, we would expect at least one tracking methodology to identify an extreme seed year.

We then incorporate explicitly tracked seeds into the TC proxy, replacing SPI with observed seed count to compute $N_{TC} \approx \text{Seeds} \times P(\Lambda)$, where $P(\Lambda)$ is derived from seasonal monthly ERA5 conditions. This modified proxy reproduces a substantial portion of observed interannual variability (correlations $r = 0.63$–0.69) and successfully captures both inactive and active years such as 2005 and 2010. Yet across all three seed-tracking methodologies, the proxy converges on a moderately active 2020 season of roughly twelve storms, below the observed 23. Thus, even when incorporating explicitly tracked seed disturbances at six-hourly resolution, the observed large-scale atmospheric conditions in 2020 do not appear sufficient to explain the record-breaking season, further suggesting an important role for subseasonal internal atmospheric variability.

4. Discussion

This study examines the apparent unpredictability of the hyperactive 2020 Atlantic TC season given the observed SST boundary conditions, during which activity across all intensity bins exceeded the ensemble spread of state-of-the-art GFDL atmosphere-only climate models forced with observed SSTs (Fig. 1). We considered two broad classes of hypotheses to explain the discrepancy between observations and model simulations. The first posits that model or observational deficiencies prevented the ensembles from reproducing a hyperactive outcome comparable to that observed. The second considers whether the 2020 season represented a dynamically plausible but

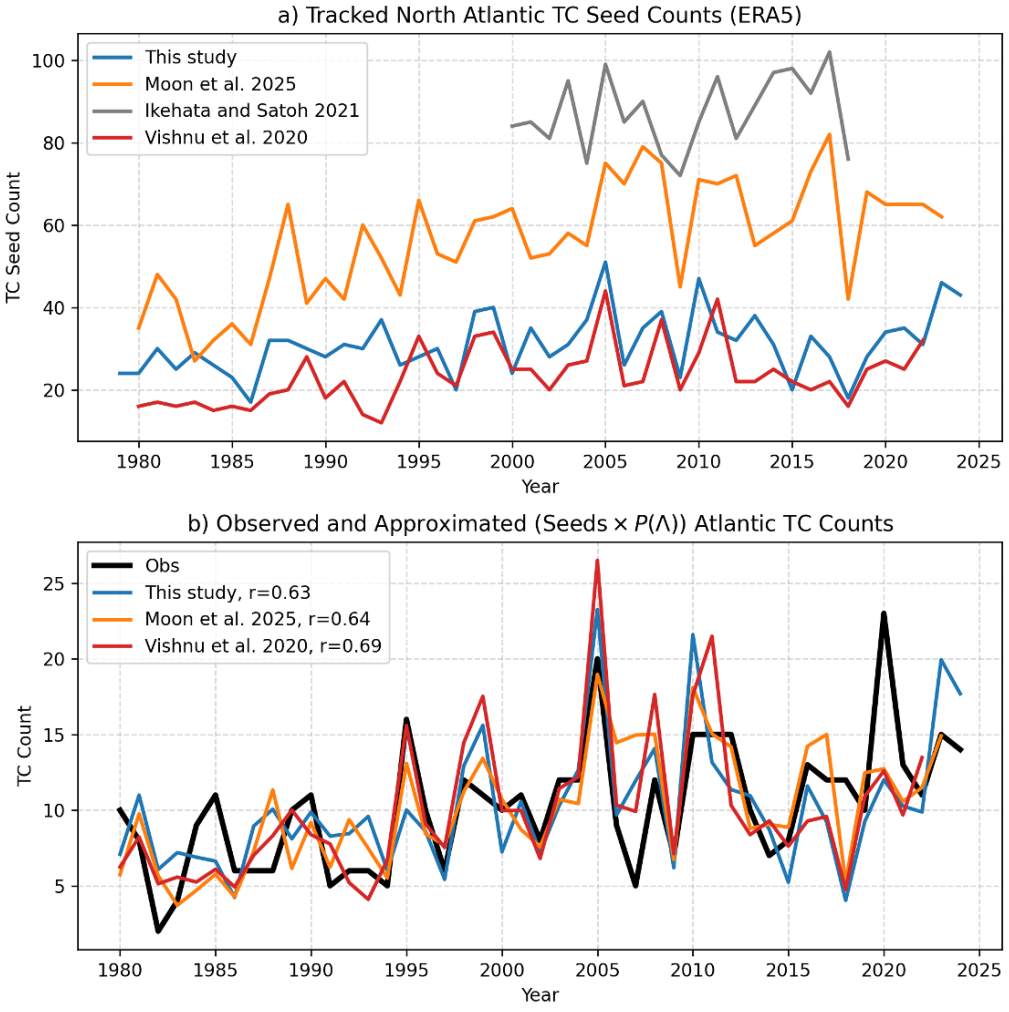

552 FIG. 5. (a) Tracked Atlantic tropical cyclone (TC) seed counts from the ERA5 dataset using the methods
553 described in Section 2 (blue; 1979–2024), from Moon et al. (2025) (orange; 1980–2023), Ikehata and Satoh
554 (2021) (gray; 2000–2018), and Vishnu et al. (2020) (red; 1980–2022).(b) Observed annual Atlantic TC counts
555 (black) and approximated annual TC frequencies derived from seed counts (Seeds $\times P(\Lambda)$), where $P(\Lambda)$ represents
556 the transition probability estimated from seasonally and MDR-averaged monthly ERA5 conditions. Seed counts
557 are obtained following the respective tracking methods in Section 2 (blue; 1980–2024), Moon et al. (2025)
558 (orange; 1980–2023), and Vishnu et al. (2020) (red; 1980–2022). Approximated TC counts are scaled by a
559 multiplicative factor so that their mean matches the observed mean. Correlation coefficients between observed
560 and approximated TC counts for each seed dataset are shown in the upper-left corner of panel (b).

low-probability realization under the observed SST forcing that could not have been captured by the limited ensemble sizes of AM2.5-C360 and HiRAM.

After systematically evaluating four hypotheses within the first category using dynamical and statistical–dynamical models, we find little evidence supporting model or observational failure. Moreover, analysis of the large-scale environmental conditions using the theoretical framework of Hsieh et al. (2020) indicates that 2020 did not exhibit exceptionally favorable environmental conditions for a record-breaking season. Collectively, these results suggest that the SST-forced atmosphere-only models did not fundamentally fail by simulating only moderate activity, because the large-scale state itself was not strongly conducive to hyperactivity. Instead, we hypothesize that an unusually favorable realization of internal atmospheric variability likely enhanced the 2020 TC activity above expected levels from mean conditions alone.

Additional features of the 2020 season are consistent with enhanced internal variability with limited predictability from observed SST boundary conditions. The season included a large number of relatively weak storms compared with other hyperactive years such as 2005 and 2010 (Fig. S5). These characteristics are consistent with a scenario in which weather-scale variability amplified seasonal counts beyond what would be anticipated from large-scale environmental forcing alone.

To test whether 2020 could plausibly represent a rare but dynamically consistent outcome under the observed SST forcing, we generated a 1,000-member ensemble for 2020 using the ACE2 DL model forced with observed SSTs and applied the statistical–dynamical model of Vecchi et al. (2011) to the same SST forcing to estimate the full distribution of possible seasonal outcomes. These distributions indicate that a 23-TC season corresponds to an event with an approximate probability of 0.1–0.5% under the observed 2020 SST forcing. While such an outcome is extremely unlikely in any individual year, the probability of observing at least one 0.5% event over a 45-year period is approximately 20%. Thus, the hyperactive 2020 season is best interpreted as a rare but dynamically plausible realization rather than clear evidence of systematic model failure. More broadly, it highlights both the limited predictability of extreme seasonal TC outcomes from monthly SST boundary conditions alone and the difficulty of adequately sampling the observed tail risk with the small (five–ten member) ensembles of AM2.50-C360 and HiRAM.

Seasonal forecasts from both dynamical systems (Murakami et al. 2025) and DL-based models (Zhang et al. 2025a) similarly underestimated the realized 2020 storm frequency, with the observed

counts falling outside their ensemble ranges. Although the forecast systems in these studies performed reasonably well in predicting seasonal accumulated cyclone energy (ACE), which reflects the combined effects of storm frequency, intensity, and duration, our focus here is specifically on the unprecedented storm counts across intensity categories rather than the characteristics of individual storms or ACE, which fall outside the scope of this study. While seasonal outlooks generally anticipated an active season, none suggested the degree of hyperactivity that ultimately occurred. For example, NOAA's 2020 seasonal outlook assigned a 60% probability to an above-normal season, indicating elevated risk but not a definitive expectation of extreme activity. Moreover, although several forecasting systems predicted active conditions, the observed storm counts exceeded the forecast ranges across multiple intensity bins (Table S1). Because these outlooks typically provide qualitative count ranges rather than full probability distributions, they do not allow direct estimation of the probability of an outcome as extreme as the observed 2020 season.

To address this limitation, we estimate the likelihood of the observed 2020 storm count by applying May-initialized North American Multi-Model Ensemble (NMME) forecast SSTs to the statistical–dynamical model of Vecchi et al. (2011), following the methodology of Villarini et al. (2019). Consistent with other seasonal outlooks, these SST forecasts generally predicted a moderately active season relative to their historical forecasts, largely reflecting favorable Atlantic-to-tropical SST gradients. However, none indicated a record-breaking hyperactive outcome. This is consistent with Bell et al. (2021), who similarly found that relative Atlantic SST anomalies in 2020 were locally elevated but not as extreme as in seasons such as 1999, 2005, or 2010. Under the NMME SST forecasts, the observed 23-storm season corresponds to an event with an estimated probability ranging from less than 0.05% to 4.5%, depending on the forecast model (Fig. S9). The models assigning the highest probabilities (1–4.5%) exhibited warm biases in Atlantic MDR SSTs relative to observations (Figs. S7 and S8), effectively creating boundary conditions more favorable for TC activity than those that actually occurred. Thus, although these biased forecasts made the observed hyperactivity appear more likely, even they assigned less than a 5% probability to a season as extreme as 2020. In other words, even with biased, overly favorable SST conditions, the models did not suggest that record-breaking hyperactivity was a likely outcome.

Finally, although Klotzbach et al. (2022) argued that aspects of the elevated late-season activity in 2020 may have been anticipated using large-scale predictors, that analysis focused primarily

on intensity-related metrics such as accumulated cyclone energy and rapid intensification. To our knowledge, the seasonal predictability of the realized storm frequency itself given observed SST forcing has not previously been examined.

5. Conclusions

The evidence presented here supports the conclusion that the observed 2020 SST boundary conditions did not confer strong predictability for the hyperactive outcome. Instead, the record-breaking season was likely a rare realization of internal atmospheric variability superimposed on a moderately favorable large-scale environmental state. Further, our results support the conclusion that the hyperactive 2020 season can be understood as an unlikely outcomes that even a well-calibrated system, like the modeling systems used in this study, will exhibit. Such rare but dynamically plausible events may be fundamentally difficult to capture with small ensemble sizes, even when the models themselves are performing appropriately. This interpretation of the 2020 season does not exclude the possibility that additional mechanisms not examined here contributed to the observed activity. Future observations, modeling advances, or reanalysis improvements could alter this assessment. New evidence could emerge to support hypotheses one through four, for which we were not able to find compelling support in the results presented here. Moreover, if similar large discrepancies between observations and model ensembles become more frequent, reassessment of model calibration and structural assumptions would be warranted.

Our findings have several broader implications. First, the 2020 season occurs at the end of the recent historical record and is anomalously hyperactive, which makes it disproportionately influential in linear trend estimates (Fig. S10). Because trend calculations are especially sensitive to extreme values near the endpoints of a time series, the inclusion of 2020 amplifies the estimated 1980–2024 increase in Atlantic TC, hurricane, and major hurricane activity by approximately six storms per century for TCs, two storms per century for hurricanes, and one storm per century for major hurricanes. Although removing 2020 does not reverse the positive sign of the TC or major hurricane trends at the 95% confidence level, it substantially reduces their magnitudes. In contrast, for hurricanes, excluding 2020 causes the 95% confidence interval to cross zero, implying that the statistical evidence for a positive hurricane trend weakens considerably in its absence. This behavior indicates that 2020 acts as a high-leverage endpoint in the regression and exerts

disproportionate influence on the inferred trends. This sensitivity is important because projected changes in TC frequency under anthropogenic forcing remain an open and actively debated research question (e.g., Knutson et al. 2020; Sobel et al. 2021). If the exceptional 2020 season primarily reflects internal variability, such as subseasonal fluctuations or weather-scale noise, then its strong influence on multidecadal trends complicates the interpretation of those trends as indicators of externally forced climate change. These results highlight the need for caution when drawing conclusions about long-term TC trends from relatively short observational records, particularly when extreme endpoint seasons exert substantial leverage on estimated changes. Our findings therefore stress the importance of employing statistical measures more resistant to the influence of outliers, such as the median of pairwise slopes (Lazante 1996).

Next, this study is one of many to highlight the value of very large ensembles (e.g., Mahesh et al. 2025a,b). We found that the five to ten member size from the dynamical models used in this study is not sufficient to study a full distribution of potential outcomes, especially given that the observed record is expected to exceed the ensemble spread across a multidecadal historical record several times. Traditional modeling efforts leverage a relatively small ensemble size. For example, the seasonal forecasting systems in Murakami et al. (2025) and Zhang et al. (2025a) use ensembles of ten to fifteen members, and operational global meteorological agencies generally use no more than a few dozen. In contrast, this study employs 1,000 ensemble members of the ACE2 DL model to assess the full distribution of outcomes for 2020 Atlantic TC season. By leveraging the computational efficiency of DL–based weather and climate emulators, future forecast systems should continue to incorporate much larger ensembles and explicitly consider tail risks, rather than depending primarily on ensemble means, to prepare for low-probability but high-impact events.

In summary, the 2020 Atlantic TC season appears consistent with a rare realization within a probabilistic framework rather than a systemic model failure. Even well-calibrated forecasting systems will occasionally encounter extreme outcomes like the 2020 season. Recognizing and quantifying this possibility is essential for interpreting past extremes and preparing for future risk.

Acknowledgments. We thank Greg Hakim, Gabriele Villarini, Stephan Fueglistaler, Hiro Murakami, Aidan Mahoney, and Gabe Rios for helpful discussion and comments, and we thank Spencer Clark at Ai2 and Colm Talbot and Mattie Niznik at Princeton Research Computing for their assistance in running the ACE2 model. We would like to thank Chanyoung Park for helping prepare the MERRRA-2 aerosol files in a format compatible with the models used in this study. This work has been supported by the Carbon Mitigation Initiative at Princeton University, funded by BP. E.L. was supported by the National Science Foundation Graduate Research Fellowship. This work was funded, in part, by the Heising-Simons Foundation Grant 2023-4720. The simulations were performed on computational resources managed and supported by Princeton Research Computing, a consortium of groups including the Princeton Institute for Computational Science and Engineering, the Office of Information Technology's High Performance Computing Center, and the Visualization Laboratory at Princeton University.

Data availability statement. Source code of the HiRAM model is available from `https://www.gfdl.noaa.gov/HiRAM-quickstart`, and the source code of the ACE2 model is available from `https://github.com/ai2cm/ace`. The forcing data and initial conditions for the ACE2 model are available from `https://huggingface.co/allenai/ACE2-ERA5/tree/main/initial_conditions`. ERA5 data are available from `https://cds.climate.copernicus.eu/datasets/reanalysis-era5-pressure-levels-monthly-means?tab=overview`, and MERRA2 data are available from `https://gmao.gsfc.nasa.gov/gmao-products/merra-2/data-access_merra-2/`. The OISST data are available from `https://www.ncei.noaa.gov/products/optimum-interpolation-sst`, the HadISST data are available from `https://www.metoffice.gov.uk/hadobs/hadisst/`, and the ERSST data are available from `https://www.ncei.noaa.gov/products/extended-reconstructed-sst`. The code to compute the components of the tropical cyclone activity proxy are available from `https://github.com/tlhsieh/tropical_cyclone_seeds` and `https://github.com/wy2136/wython/tree/main/xtci/shared`. The TC seed dataset of Ikehata and Satoh (2021) is available at `https://doi.org/10.5281/zenodo.5136292`, the low pressure system dataset of Vishnu et al. (2020) is available at `https://portal.nersc.gov/cfs/m3310/VishnuEtAl_TrackDataset/`, and the seed dataset of Moon et al. (2025) is available at `https://doi.org/10.5281/zenodo.15227119`. The code to run one year's 1,000-member ensemble and process the

output, and track TCs is available at `https://github.com/emmalevin/ACE2_1000`. TC track data and monthly mean environmental conditions generated from the ACE2 1,000 member ensemble are available at the Zenodo repository: `https://doi.org/10.5281/zenodo.19456833`.

References

Bell, G. D., M. Rosencrans, E. S. Blake, C. W. Landsea, H. Wang, S. B. Goldenberg, and R. J. Pasch, 2021: State of the climate in 2020: Tropical cyclones—atlantic basin. *Bulletin of the American Meteorological Society*, **102 (8)**, S224–S230, https://doi.org/10.1175/BAMS-D-21-0093.1.

Bi, K., L. Xie, H. Zhang, X. Chen, X. Gu, and Q. Tian, 2023: Accurate medium-range global weather forecasting with 3d neural networks. *Nature*, **619 (7970)**, 533–538, https://doi.org/10.1038/s41586-023-06185-3.

Chan, D., G. A. Vecchi, W. Yang, and P. Huybers, 2021: Improved simulation of 19th- and 20th-century north atlantic hurricane frequency after correcting historical sea surface temperatures. *Science Advances*, **7 (26)**, eabg6931, https://doi.org/10.1126/sciadv.abg6931.

Chen, J.-H., and S.-J. Lin, 2011: The remarkable predictability of interannual variability of atlantic hurricanes during the past decade. *Geophysical Research Letters*, **38 (11)**, L11 804, https://doi.org/10.1029/2011GL047629.

Chen, J.-H., and S.-J. Lin, 2013: Seasonal predictions of tropical cyclones using a 25-km-resolution general circulation model. *Journal of Climate*, **26 (2)**, 531–543, https://doi.org/10.1175/JCLI-D-12-00061.1.

Chen, L., X. Zhong, F. Zhang, Y. Cheng, Y. Xu, Y. Qi, and H. Li, 2023: Fuxi: A cascade machine learning forecasting system for 15-day global weather forecast. *npj Climate and Atmospheric Science*, **6 (1)**, 190, https://doi.org/10.1038/s41612-023-00512-1.

Chien, M.-T., E. A. Barnes, and E. D. Maloney, 2025: Modulation of tropical cyclogenesis on subseasonal-to-interannual timescales in the deep-learning climate emulator ace2. *Machine Learning: Earth*, **1 (1)**, 015 008, https://doi.org/10.1088/3049-4753/adfd61.

Diamond, M. S., 2023: Detection of large-scale cloud microphysical changes within a major shipping corridor after implementation of the international maritime organization 2020 fuel

sulfur regulations. *Atmospheric Chemistry and Physics*, **23 (14)**, 8259–8269, https://doi.org/10.5194/acp-23-8259-2023.

Eusebi, R., W. Yang, G. A. Vecchi, and S. Fueglistaler, 2025a: Statistical modeling of north atlantic hurricane frequency and the impact and role of patterned warming. *Journal of Climate*, **38 (19)**, 5391–5410, https://doi.org/10.1175/JCLI-D-24-0647.1.

Eusebi, R., W. Yang, G. A. Vecchi, and S. Fueglistaler, 2025b: Statistical modeling of north atlantic hurricane frequency and the impact and role of patterned warming. *Journal of Climate*, **38 (19)**, 5391–5410, https://doi.org/10.1175/JCLI-D-24-0647.1.

Gao, K., J.-H. Chen, L. Harris, Y. Sun, and S.-J. Lin, 2019: Skillful prediction of monthly major hurricane activity in the north atlantic with two-way nesting. *Geophysical Research Letters*, **46 (16)**, 10 098–10 107, https://doi.org/10.1029/2019GL083526.

Gelaro, R., and Coauthors, 2017: The modern-era retrospective analysis for research and applications, version 2 (MERRA-2). *Journal of Climate*, **30 (14)**, 5419–5454, https://doi.org/10.1175/JCLI-D-16-0758.1.

Gneiting, T., F. Balabdaoui, and A. E. Raftery, 2007: Probabilistic forecasts, calibration and sharpness. *Journal of the Royal Statistical Society: Series B (Statistical Methodology)*, **69 (2)**, 243–268, https://doi.org/10.1111/j.1467-9868.2007.00587.x.

Hamill, T. M., 2001: Interpretation of rank histograms for verifying ensemble forecasts. *Monthly Weather Review*, **129 (3)**, 550–560, https://doi.org/10.1175/1520-0493(2001)129⟨0550:IORHFV⟩2.0.CO;2.

Hersbach, H., and Coauthors, 2020: The ERA5 global reanalysis. *Quarterly Journal of the Royal Meteorological Society*, **146 (730)**, 1999–2049, https://doi.org/10.1002/qj.3803.

Hsieh, T.-L., G. A. Vecchi, W. Yang, I. M. Held, and S. T. Garner, 2020: Large-scale control on the frequency of tropical cyclones and seeds: a consistent relationship across a hierarchy of global atmospheric models. *Climate Dynamics*, **55 (11)**, 3177–3196, https://doi.org/10.1007/s00382-020-05446-5.

Huang, B., C. Liu, V. Banzon, E. Freeman, G. Graham, B. Hankins, T. Smith, and H.-M. Zhang, 2021: Improvements of the daily optimum interpolation sea surface temperature (doisst) version 2.1. *Journal of Climate*, **34 (8)**, 2923–2939, https://doi.org/10.1175/JCLI-D-20-0166.1.

Huang, B., and Coauthors, 2017: Extended reconstructed sea surface temperature, version 5 (ersstv5): Upgrades, validations, and intercomparisons. *Journal of Climate*, **30 (20)**, 8179–8205, https://doi.org/10.1175/JCLI-D-16-0836.1.

Ikehata, K., and M. Satoh, 2021: Climatology of tropical cyclone seed frequency and survival rate in tropical cyclones. *Geophysical Research Letters*, **48 (18)**, e2021GL093 626, https://doi.org/10.1029/2021GL093626.

Jordan, G., and M. Henry, 2024: IMO2020 regulations accelerate global warming by up to 3 years in UKESM1. *Earth's Future*, **12 (8)**, e2024EF005 011, https://doi.org/10.1029/2024EF005011.

Klotzbach, P. J., S. G. Bowen, R. Pielke, and M. Bell, 2018: Continental u.s. hurricane landfall frequency and associated damage: Observations and future risks. *Bulletin of the American Meteorological Society*, **99 (7)**, 1359–1376, https://doi.org/10.1175/BAMS-D-17-0184.1.

Klotzbach, P. J., and Coauthors, 2022: A hyperactive end to the atlantic hurricane season october–november 2020. *Bulletin of the American Meteorological Society*, **103 (1)**, S1–S28, https://doi.org/10.1175/BAMS-D-20-0312.1.

Knutson, T., and Coauthors, 2020: Tropical cyclones and climate change assessment: Part II: Projected response to anthropogenic warming. **101 (3)**, E303–E322, https://doi.org/10.1175/BAMS-D-18-0194.1.

Kochkov, D., and Coauthors, 2024: Neural general circulation models for weather and climate. *Nature*, **632 (8027)**, 1060–1066, https://doi.org/10.1038/s41586-024-07744-y.

Kortum, G., G. A. Vecchi, T.-L. Hsieh, and W. Yang, 2024: Influence of weather and climate on multidecadal trends in atlantic hurricane genesis and tracks. *Journal of Climate*, **37 (5)**, 1501–1522, https://doi.org/10.1175/JCLI-D-23-0088.1.

Lam, R., and Coauthors, 2023: Learning skillful medium-range global weather forecasting. *Science*, **382 (6677)**, 1416–1421, https://doi.org/10.1126/science.adi2336.

Landsea, C. W., G. A. Vecchi, L. Bengtsson, and T. R. Knutson, 2010a: Impact of duration thresholds on atlantic tropical cyclone counts. **23 (10)**, 2508–2519, https://doi.org/10.1175/2009JCLI3034.1.

Landsea, C. W., G. A. Vecchi, L. Bengtsson, and T. R. Knutson, 2010b: Impact of duration thresholds on atlantic tropical cyclone counts. https://doi.org/10.1175/2009JCLI3034.1.

Lang, S., and Coauthors, 2024: AIFS: ECMWF's data-driven forecasting system. URL https://arxiv.org/abs/2406.01465, arXiv preprint, https://doi.org/10.48550/arXiv.2406.01465, 2406.01465.

Lazante, J. R., 1996: Resistant, robust and non-parametric techniques for the analysis of climate data: Theory and examples, including applications to historical radiosonde station data. **16 (11)**, 1197–1226, https://doi.org/10.1002/(SICI)1097-0088(199611)16:11⟨1197::AID-JOC89⟩3.0.CO;2-L.

Levin, E. L., G. A. Vecchi, and W. Yang, 2026: Influence of sea surface temperature patterns and mean warming on past and future atlantic tropical cyclone activity. *Journal of Climate*, **39 (10)**, 3735–3758, https://doi.org/10.1175/JCLI-D-25-0635.1.

Mahesh, A., and Coauthors, 2025a: Huge ensembles–part 1: Design of ensemble weather forecasts using spherical fourier neural operators. *Geoscientific Model Development*, **18 (17)**, 5575–5603, https://doi.org/10.5194/gmd-18-5575-2025.

Mahesh, A., and Coauthors, 2025b: Huge ensembles–part 2: Properties of a huge ensemble of hindcasts generated with spherical fourier neural operators. *Geoscientific Model Development*, **18 (17)**, 5605–5633, https://doi.org/10.5194/gmd-18-5605-2025.

Menemenlis, S., G. A. Vecchi, W. Yang, S. Fueglistaler, and S. P. Raghuraman, 2025: Consequential differences in satellite-era sea surface temperature trends across datasets. *Nature Climate Change*, **15 (8)**, 897–903, https://doi.org/10.1038/s41558-025-02362-6.

Moon, J., D. Kim, A. A. Wing, S. J. Camargo, G. N. Emlaw, J. C. Starr, and D.-H. Cha, 2025: Tropical cyclone seed disturbances in ERA5. *Journal of Climate*, **38 (18)**, 4625–4639, https://doi.org/10.1175/JCLI-D-24-0291.1.

Murakami, H., 2022: Substantial global influence of anthropogenic aerosols on tropical cyclones over the past 40 years. *Science Advances*, **8 (19)**, eabn9493, https://doi.org/10.1126/sciadv.abn9493.

Murakami, H., 2024: Effect of regional anthropogenic aerosols on tropical cyclone frequency of occurrence. *Geophysical Research Letters*, **51 (21)**, e2024GL110 443, https://doi.org/10.1029/2024GL110443.

Murakami, H., T. L. Delworth, N. C. Johnson, F. Lu, C. E. McHugh, and L. Jia, 2025: Seasonal forecasts of tropical cyclones using GFDL SPEAR and HiFLOR-s. *Journal of Climate*, **38 (9)**, 3601–3620, https://doi.org/10.1175/JCLI-D-24-0356.1.

Pielke, R. A., J. Gratz, C. W. Landsea, D. Collins, M. A. Saunders, and R. Musulin, 2008: Normalized hurricane damage in the united states: 1900–2005. **9 (1)**, 29–42, https://doi.org/10.1061/(ASCE)1527-6988(2008)9:1(29).

Schneider, D. P., C. Deser, J. Fasullo, and K. E. Trenberth, 2013: Climate data guide spurs discovery and understanding. *Eos, Transactions American Geophysical Union*, **94 (13)**, 121–122, https://doi.org/10.1002/2013EO130001.

Sobel, A. H., A. A. Wing, S. J. Camargo, C. M. Patricola, G. A. Vecchi, C. Lee, and M. K. Tippett, 2021: Tropical cyclone frequency. *Earth's Future*, **9 (12)**, e2021EF002 275, https://doi.org/10.1029/2021EF002275.

Tang, B., and K. Emanuel, 2010: Midlevel ventilation's constraint on tropical cyclone intensity. *Journal of the Atmospheric Sciences*, **67 (6)**, 1817-1830, https://doi.org/10.1175/2010JAS3318.1.

Tang, B., and K. Emanuel, 2012: A ventilation index for tropical cyclones. *Bulletin of the American Meteorological Society*, **93 (12)**, 1901-1915, https://doi.org/10.1175/BAMSD1100165.1.

Ullrich, P. A., and C. M. Zarzycki, 2017: TempestExtremes: a framework for scale-insensitive pointwise feature tracking on unstructured grids. *Geoscientific Model Development*, **10 (3)**, 1069–1090, https://doi.org/10.5194/gmd-10-1069-2017.

Vecchi, G. A., and B. J. Soden, 2007: Effect of remote sea surface temperature change on tropical cyclone potential intensity. *Nature*, **450 (7172)**, 1066–1070, https://doi.org/10.1038/nature06423.

Vecchi, G. A., and G. Villarini, 2014: Next season's hurricanes. *Science*, **343 (6171)**, 618–619, https://doi.org/10.1126/science.1247759.

Vecchi, G. A., M. Zhao, H. Wang, G. Villarini, A. Rosati, A. Kumar, I. M. Held, and R. Gudgel, 2011: Statistical–dynamical predictions of seasonal north atlantic hurricane activity. *Monthly Weather Review*, **139 (4)**, 1071–1087, https://doi.org/10.1175/2010MWR3499.1.

Vecchi, G. A., and Coauthors, 2019: Tropical cyclone sensitivities to co2 doubling: roles of atmospheric resolution, synoptic variability and background climate changes. *Climate Dynamics*, **53 (9)**, 5999–6033, https://doi.org/10.1007/s00382-019-04913-y.

Villarini, G., B. Luitel, G. A. Vecchi, and J. Ghosh, 2019: Multi-model ensemble forecasting of north atlantic tropical cyclone activity. *Climate Dynamics*, **53 (11–12)**, 7461–7477, https://doi.org/10.1007/s00382-016-3360-z.

Villarini, G., G. A. Vecchi, T. R. Knutson, M. Zhao, and J. A. Smith, 2011: North atlantic tropical storm frequency response to anthropogenic forcing: Projections and sources of uncertainty. *Journal of Climate*, **24 (13)**, 3224–3248, https://doi.org/10.1175/2011JCLI3853.1.

Villarini, G., G. A. Vecchi, and J. A. Smith, 2010: Modeling the dependence of tropical storm counts in the north atlantic basin on climate indices. https://doi.org/10.1175/2010MWR3315.1.

Vishnu, S., W. R. Boos, P. A. Ullrich, and T. A. O'Brien, 2020: Assessing historical variability of south asian monsoon lows and depressions with an optimized tracking algorithm. *Journal of Geophysical Research: Atmospheres*, **125 (15)**, e2020JD032 977, https://doi.org/10.1029/2020JD032977.

Watt-Meyer, O., and Coauthors, 2025: ACE2: Accurately learning subseasonal to decadal atmospheric variability and forced responses. *npj Climate and Atmospheric Science*, **8 (1)**, 205, https://doi.org/10.1038/s41612-025-01090-0.

Weinkle, J., C. Landsea, D. Collins, R. Musulin, R. P. Crompton, P. J. Klotzbach, and R. Pielke, 2018: Normalized hurricane damage in the continental united states 1900–2017. *Nature Sustainability*, **1 (12)**, 808–813, https://doi.org/10.1038/s41893-018-0165-2.

Yang, W., T.-L. Hsieh, and G. A. Vecchi, 2021: Hurricane annual cycle controlled by both seeds and genesis probability. *Proceedings of the National Academy of Sciences*, **118 (41)**, e2108397 118, https://doi.org/10.1073/pnas.2108397118.

Young, R., and S. Hsiang, 2024: Mortality caused by tropical cyclones in the united states. *Nature*, **635 (8037)**, 121–128, https://doi.org/10.1038/s41586-024-07945-5.

Zhang, G., M. Rao, J. Yuval, and M. Zhao, 2025a: Advancing seasonal prediction of tropical cyclone activity with a hybrid ai–physics climate model. *Environmental Research Letters*, **20 (9)**, 094 031, https://doi.org/10.1088/1748-9326/adf864.

Zhang, J., Y.-S. Chen, E. Gryspeerdt, T. Yamaguchi, and G. Feingold, 2025b: Radiative forcing from the 2020 shipping fuel regulation is large but hard to detect. *Communications Earth & Environment*, **6 (1)**, 1–11, https://doi.org/10.1038/s43247-024-01911-9.

Zhao, M., I. M. Held, S.-J. Lin, and G. A. Vecchi, 2009: Simulations of global hurricane climatology, interannual variability, and response to global warming using a 50-km resolution gcm. *Journal of Climate*, **22 (24)**, 6653–6678, https://doi.org/10.1175/2009JCLI3049.1.

Zhao, M., I. M. Held, and G. A. Vecchi, 2010: Retrospective forecasts of the hurricane season using a global atmospheric model assuming persistence of sst anomalies. *Monthly Weather Review*, **138 (10)**, 3858–3868, https://doi.org/10.1175/2010MWR3366.1.